Industrial CMOS technology for the integration of optical metrology systems (photo-ASICs)*

J Kramer** and P Seitz
Paul Scherrer Institute Zurich, Badenerstrasse 569 CH-8048 Zurich (Switzerland)

H Baltes
Swiss Federal Institute of Technology, Physical Electronics Laboratory, ETH-Honggerberg HPT, CH-8093 Zurich (Switzerland)

(Received January 7, 1992, accepted February 21, 1992)

Abstract

With 'photo-ASICs' comprising light-sensitive structures, light-emitting devices and analog and digital circuits, complete optical metrology systems can be integrated on a single chip We report the realization of key components of such photo-ASICs using an industrial IC CMOS process We achieve photodiodes with an external quantum efficiency of 50–80% in the visible spectrum and position-sensitive devices (PSDs) with a spatial non-linearity of around 0 3% We demonstrate surface-channel CCDs with a charge-transfer efficiency of 99 8% at room temperature, as well as bucket-brigade devices (BBDs) with a lower charge-transfer efficiency of 96% Light-emitting diodes (LEDs) are realized, emitting infrared light at 1160 nm (forward biased) and broadband visible yellow light with a spectral maximum at 640 nm (reverse biased) We discuss simple applications of passive photo-ASICs, such as a centroid detector, a 3-D camera, a motion detector and a focus sensor, used to obtain a relative measure for the local focus of an optically imaged scene, for example, in a photographic camera

1. Introduction

It is well known that radiation with photonic energies exceeding the band gap of semiconductor material generates charge carriers in the semiconductor If the same semiconductor material is used to fabricate analog and digital circuitry, it is straightforward to cointegrate analog, digital and photosensitive elements on the same chip These chips, called 'photo-ASICs', 'opto-ASICs' or, more suggestively, 'seeing chips' [1], are capable of realizing optical sensing elements and associated processing electronics on the same substrate Since modern design, layout and simulation tools are readily available for PCs and workstations at very low cost, and since many silicon foundries running standard semiconductor processes offer inexpensive multi-project wafer services, it has become possible for a wide range of researchers and engineers to exploit the potential of photo-ASICs for many practical applications This capability has been used extensively for the simulation of certain properties of biological vision systems in silicon [2, 3]

Optical metrology applications of photo-ASICs [4] have barely been broached hitherto, because the optoelectronic properties of the devices are more critical in such applications The purpose of this work is to investigate whether an industrial CMOS process (normally used for low-power low-noise analog and digital circuits for battery-driven devices such as hearing aids) is suitable to realize photo-ASICs for integrated optical metrology

The CMOS process chosen is SACMOS-3 offered by FASELEC [5], an established, simple and inexpensive silicon p-well process (single poly, single metal) with 3 μm design rules and self-aligned contacts This process was used to integrate prototypes with various electro-optical properties In Section 2 different types of photodiodes are discussed The good uniformity of the semiconductor layers can be inferred from the excellent linearity of a PSD (position-sensitive device), as discussed in Section 3 In Section 4 we demonstrate that it is also possible to integrate

*Paper presented at the 6th International Conference on Solid-State Sensors and Actuators (Transducers 91), San Francisco, CA, USA, June 24 28, 1991

**Author to whom correspondence should be addressed

0924-4247/92/$5 00

© 1992 — Elsevier Sequoia All rights reserved

surface-channel CCDs (charge-coupled devices) with reasonable charge-transfer efficiencies, albeit at high voltages Although silicon is an indirect band-gap material, it is feasible to integrate light sources (silicon LEDs) with the same CMOS process In Section 5 practical results for near-infrared and visible light emitters are shown Three different applications of photo-ASICs are demonstrated in Section 6, illustrating the practical use of this readily available technology for practical optical metrology applications Section 7 offers a discussion of the potential of photo-ASICs and an assessment of their future use in science and engineering

2. Photodiodes

Four different types of square pn-junction photodiodes were realized, each with an area of 100 μm × 100 μm, as illustrated in the cross sections of Fig 1 All photodiodes exhibit external quantum efficiencies between 50 and 80% in the visible, extending to the near infrared up to around 1150 nm Figure 2 shows a typical spectral response as measured for the n^-p^- diode (the left-most diode in Fig 1) The spectral oscillations are caused by optical interference at the passivation interfaces Suitable anti-reflection coatings could reduce these interference effects appreciably

Surface leakage currents are found in the $n^+p^-n^-$ structure, reducing the open-loop voltages at all light levels and reducing the short-circuit current under strong illumination This is probably caused by edge breakdown in the pn-junction's space-charge region at the surface [6] In the p^+n^- diode this was successfully avoided through the use of a p^- guard ring Dark currents of less than 1 pA at room temperature are measured for the photodiodes

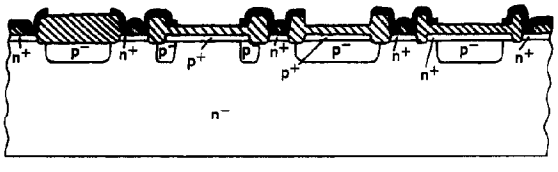

Fig 1 Cross sections of four different types of photodiodes integrated using a simple industrial CMOS process, offering one polysilicon and one metal layer Note the guard-ring in the second photodiode from the left, which successfully prevents edge breakdown and reduction of the open-loop voltage

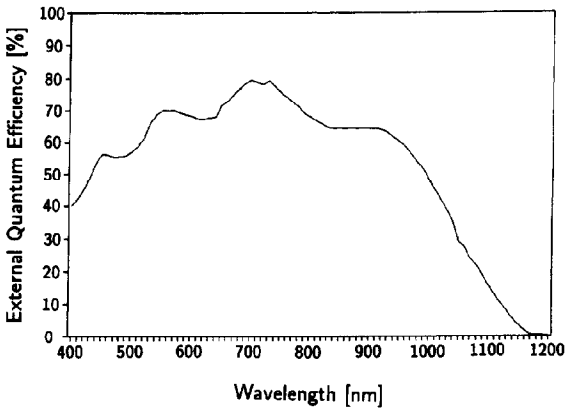

Fig 2 Absolute spectral response (external quantum efficiency) of the n^-p^- photodiode shown in Fig 1 at the left The spectral oscillations are caused by interference effects at the passivation interfaces, which could be substantially reduced with suitable anti-reflection coatings

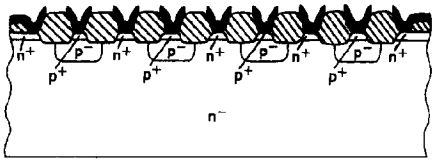

Fig 3 Lateral photodiodes, in which the width of the space-charge regions is controlled with the reverse-bias voltage In this way the photosensitive area can be controlled electrically, leading to a voltage-controlled fast aperture sensor

Figure 3 illustrates a lateral photodiode, created by a dense arrangement of predominantly vertical pn-junctions The (lateral) width of the diode's space-charge region can be adjusted with the reverse voltage In this way the photosensitive area can be changed by applying a suitable voltage Without additional masking or post-treatment of the structure, this effect amounts to about 5% in our device It is expected that this could be enhanced significantly so as to arrive at a photodetector with an electrically controlled fast aperture

3. Position-sensitive device (PSD)

It is also possible to design and fabricate lateral-effect photodiodes, also called position-sensitive devices (PSDs), with a simple CMOS process such as the one used here Since a PSD relies on the current-dividing properties of a resistive layer, the linearity with which the position of a light spot can be determined is a direct measure of the

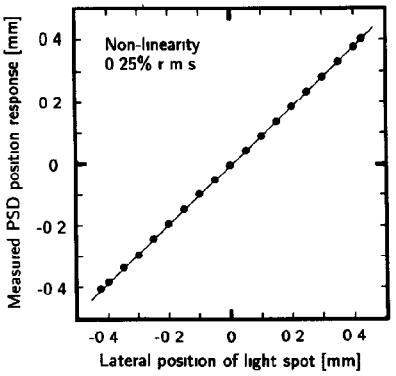

Fig 4 Geometrical linearity of a CMOS position-sensitive device (PSD) The obtained deviation from perfect linearity of 0 2% r m s is close to that achieved with the best commercially available PSDs

uniformity of the corresponding doped semiconductor layer

Our PSD is formed by a low-resistivity p^+ layer (sheet resistance 170 Ω/□) contacted at opposite edges The n^- substrate is contacted at all sides of the 0 9 mm × 0 1 mm rectangular PSD Because of the omission of a p^- guard ring, the open-loop voltages were much lower than for the p^+n^- diode described above Nevertheless, the positioning performance of this one-dimensional PSD proved to be very good A small light spot is scanned across the PSD and the position signal is recorded This position signal is given by the ratio of the difference and the sum of the output currents at the two p^+ contacts The geometrical non-linearity, illustrated in Fig 4, was typically less than 0 5%, in one device even as low as 0 2%, in the central 0 8 mm of the device This performance comes close to the one offered by commercial PSDs tuned for precision measurements

The extension of a one-dimensional PSD to a two-dimensional low-distortion PSD with switched MOSFET gates for multiplexed coordinate measurements [7] is straightforward Thus we conclude that a standard industrial CMOS process is equally well suited for high-performance two-dimensional PSDs Investigations to prove this point are in progress

4. Charge-coupled devices (CCDs) and bucket-brigade device (BBD)

Since its invention in 1970 [8], the charge-coupled device (CCD) has made a dramatic impact on solid-state image sensing and signal-processing [9] specialized CCD processes and designs have been used to realize CCD imagers with up to 4096 × 4096 pixels [10], noise levels below 0 5 electrons r m s [10] and single-channel clocking speeds exceeding 100 MHz [11] All these advances are based on the CCD's properties of offering virtually noise-free and lossless charge transfer achievable with basically very simple MOS structures Actually measured charge-transfer inefficiencies are as low as 10^{-5} per transfer

For these reasons it is of interest to investigate to what extent a standard industrial CMOS process can be used to realize CCDs and what their performance is To avoid the charge-trapping and recombination problems associated with semiconductor–oxide surfaces, almost all modern CCDs are of the buried-channel type [9] This requires an additional shallow implant, which is optionally available in some specialized CCD-CMOS processes, e g , the 2 μm n-well FORESIGHT process [12], but not in a normal CMOS process This implies that a surface-channel CCD architecture must be employed Since it has been shown that charge-transfer efficiencies of 99 98% and more are also achievable in surface-channel CCDs [13], this is not a serious limitation except in high-performance imaging applications

While modern CCD processes use overlapping electrodes to avoid parasitic channel potentials (barriers or wells), the practical results shown in ref 13 and the detailed examination of non-overlapping electrode effects in ref 14 make it clear that CCDs that work well can also be obtained with non-overlapping electrodes, albeit at the expense of higher electrode potentials for equal performance This means that CCDs are also practical with simple and low-cost CMOS processes, such as the one investigated in the present work, offering only one level of polysilicon for non-overlapping electrodes

A simple linear CCD structure realized with the described SACMOS-3 process consists of a three-phase arrangement of two-level polysilicon electrodes with a size of 36 μm × 36 μm As dictated by the design rules, a 3 μm interelectrode spacing had to be used With such a large spacing, high voltages are expected for reasonable charge-transfer efficiencies [13, 14] in our experiments, the best results are obtained with clock levels of −11 V and −26 V with respect to the substrate

The clock frequency employed is low, namely 6 6 kHz, because all clocking patterns are generated by a PC in real time for simplicity

In an initial experiment the charge transfer showed a strong dependence on charge-signal level, with typical values for the charge-transfer efficiency of 95–98% As a means of injecting charge into the CCD, we either project a spot of red light from a modulated LED onto the CCD, or we apply a pulse at the CCD's input diode When carriers are generated only under one electrode (in one potential well) the detected amount of charge in the subsequent potential wells is independent of the number of generated carriers, as long as it exceeds a certain limit This suggests the presence of a certain number of surface states, capable of trapping carriers and partly re-emitting them into succeeding charge packets This problem is solved by the so-called 'fat zero' technique, consisting of the introduction of a fixed bias charge into each charge packet in order to keep the surface states permanently occupied With this signal 'offsetting' technique the trapping of signal charge is largely avoided In our experiment a constant bias of −0 75 V at the input diode increases the charge-transfer efficiency to 99 8%

With a modern CMOS process exhibiting minimum feature sizes of around one micron or smaller, interelectrode spacings can be reduced substantially This leads to reduced voltage requirements, and possibly to better performance [14] It is expected that surface-channel CCDs manufactured in this way can be of interest for small-area image sensing and 'seeing chips' [15], monolithic combinations of image sensors and CMOS analog and digital image-processing circuitry

A similar structure to a CCD is the so-called bucket-brigade device (BBD) [16] Like a CCD, the BBD is a charge-transfer device, but it is essentially an MOS device fully compatible with a CMOS process, requiring only simple clocking schemes and non-critical output drivers

The linear BBD realized consists of 16 metal electrodes (32 μm × 36 μm area each) and polysilicon gates to provide tetrode isolations for improved performance as described in ref 17 a two-level two-phase clock and d c biased polysilicon gates separating neighbouring electrodes are used Nevertheless, the measured charge-transfer efficiency is only slightly above 96% with the clocks operating between −11 5 V and 3 5 V at 6 6 kHz and the d c bias gates held at −6 5 V This disappointing result, although not fully understood, reproduces the findings of other researchers that CCDs generally perform better than comparable BBDs [18]

5. Infrared and visible light emission from silicon LEDs

Since silicon is an indirect band-gap semiconductor with an energy gap of 1 1 eV, it is generally assumed that (i) silicon is a very inefficient emitter of light, and (ii) light emission is restricted to the near infrared where silicon is re-absorbing very inefficiently In contrast to these widely held views, we demonstrate that infrared and visible light emission from silicon is practical and that pertinent devices can be realized inexpensively by industrial CMOS process

Although the radiative recombination probability B of a direct band-gap semiconductor such as GaAs is more than four orders of magnitude larger than that of silicon [19], the higher carrier concentrations n and p in silicon at room temperature lead to a radiative recombination rate R

$$R = Bnp = Bn_i^2 \tag{1}$$

for thermal equilibrium that is two orders of magnitude *higher* in silicon than in GaAs [19] For this reason silicon can be expected to provide a light emitter with reasonable efficiency The energy gap of 1 1 eV implies that light emission will be in the near infrared, i e the spectrum will exhibit a maximum at a wavelength slightly above 1100 nm

Using the above CMOS process, we fabricated an interdigitated diode structure, consisting of 3 μm wide and 0 5 μm deep fingers of a metal-covered n^+-implant in a p-well The p-well is contacted with 3 μm wide and 0 6 μm deep fingers of a metal-covered p^+-implant, separated from the n^+-fingers by the minimum dimension of the process of 3 μm Carrier concentrations in the different regions were 3×10^{19} for the n^+ implant, 10^{19} for the p^+ contact and $1\,5 \times 10^{15}$ for the p-well This structure with active dimensions of 70 μm × 100 μm, illustrated in Fig 5(a), acts as a light-emitting diode (LED) for the near infrared when it is forward biased Typical emission spectra as measured with a Fourier transform spectrometer are shown in Fig 6 As expected, the maximum

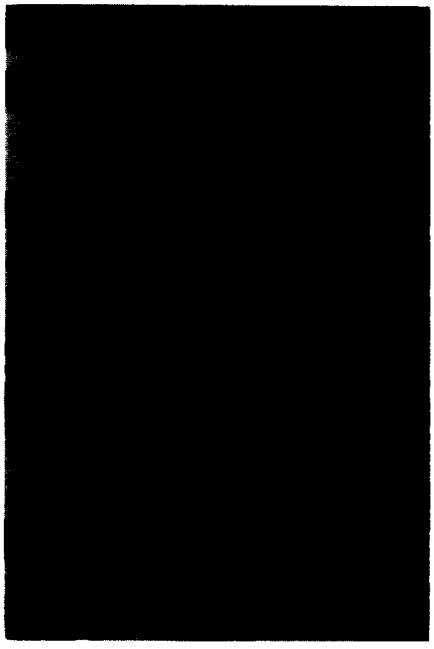

(a)

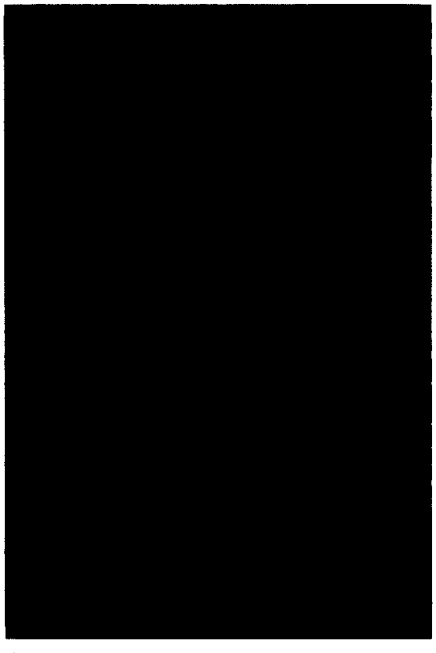

(b)

Fig 5 Interdigitated CMOS silicon LED, capable of emitting IR light and visible light The silicon LED, 70 μm × 100 μm in size, is situated between two bonding pads through which it is powered (a) Micrographic view of the silicon LED emitting visible (whitish-yellow) light spots taken with a standard black-and-white film The surrounding area of the silicon LED is illuminated by the microscope lamp (b) Same view, but with the microscope lamp switched off Note the reflexes of the generated light spots in the bonding balls

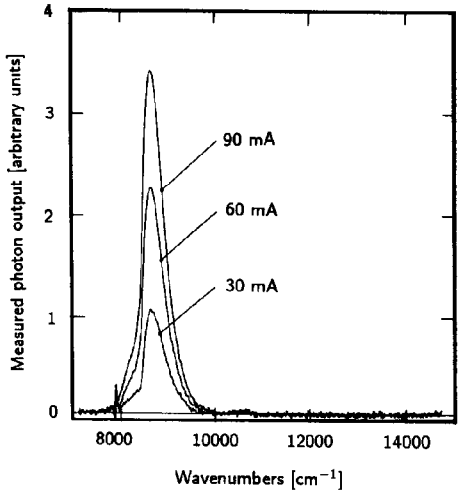

Fig 6 Infrared spectrum of the silicon LED operated in forward bias, as measured with a Fourier transform spectrometer The spectrum is centred at 1160 nm (as expected from theory) with a FWHM of around 70 nm

emission occurs at an energy of 1 07 eV, corresponding to an emission wavelength of 1160 nm

From our quantitative measurements of total emitted optical power, we estimate that the quantum efficiency of our silicon IR-LED is almost 10^{-4} and only weakly dependent on the current/voltage settings used This value is achieved with a simple diode structure using a standard industrial CMOS process, proving that silicon IR-LEDs are feasible even with non-optimized processes

As expected from theory, the spectrum of Fig 6 does not contain visible light emission Nevertheless, it was observed already in 1955 that silicon diodes *can* emit visible light if they are operated in controlled breakdown [20–22] This effect, albeit not widely known, has also been used for an industrial application, namely exposing digits onto photographic film [23] Recently this topic has been re-investigated [24], with the aim of monolithic silicon opto-coupler applications

The same CMOS-fabricated silicon LED as described above can be used to demonstrate visible light emission from silicon since the p-well is so lightly doped, a relatively high reverse voltage of 25 V is required to drive the diode into controlled avalanche breakdown [25] Figure 5(b), taken with ordinary black-and-white film through a microscope, illustrates that visible light is emitted, which is easily perceived as being of whitish-yellow colour with the unaided eye As described in ref

20, the light is emitted at or near the junction, and it consists of small light spots whose positions do not change with time Since the apparent diameter of the spots is close to the resolution limit of the microscope used, the true spatial extent of the light spots cannot be established with the instruments at our disposal The (corrected) spectrum of the emitted light, acquired with a sensitive SPEX-100 spectrometer normally used for Raman-effect and photoluminescence measurements, is shown in Fig 7 It reveals that the emitted light has a distinct maximum at around 650 nm This is in remarkable contrast to published spectra of visible light emission in silicon [20–24], which show no pronounced peak below 1100 nm It is not understood yet what causes this discrepancy, but a spectrum such as the one in Fig 7 is highly desirable because it represents a perfect match to the absorption characteristics of silicon

Quantitative measurements indicate that the above CMOS silicon LED emits visible and near-IR light with an efficiency of only around 10^{-8} This efficiency is below the value given in ref 23, which is not surprising because neither the CMOS process nor our structures can be optimized for visible light emission An obvious improvement, currently under investigation, is the employment of higher dopings for n^+p^+ diodes as described in ref 24, making it possible to work with reduced breakdown voltages of around 5 V

Complete theoretical understanding of the effects involved in producing visible light from avalanche-induced hot-carrier recombination has

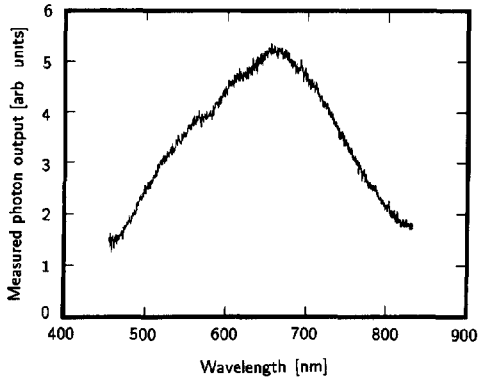

Fig 7 Visible/near infrared spectrum of the silicon LED operated in controlled avalanche breakdown This emission spectrum, measured with a sensitive SPEX-100 Raman spectrometer, is perfectly matched to the response of silicon photodetectors The emitted light is of whitish-yellow colour

not been attained yet, but first approaches have been published recently [26] Once the mechanisms for visible light emission are sufficiently well known, it may be possible technologically to optimize visible LEDs in silicon Such a development is highly desirable the integration on one silicon chip of detectors, spectrally matched light sources and analog and digital signal processing would open many new practical applications in the area of optical metrology, making low-priced custom-designed sensor solutions to optical metrology practical

We finally mention newer developments of low-dimensional ('porous') silicon structures that show high-efficiency photoluminescence in the visible [27] Such low-dimensional quantum wire or quantum dot structures must either be specially grown onto, or etched into, finished devices, and therefore are not compatible with an industrial CMOS process Nevertheless, silicon LEDs emitting in the visible have already been demonstrated using this technique [28] Possibly their luminous conversion efficiencies are substantially higher than those using the hot-charge-carrier-induced light emission discussed above

6. Applications

In the preceding Sections it was demonstrated that standard industrial CMOS technology can be employed, in principle, for the integration of complete optical metrology systems This Section is devoted to discussing three applications linked to the degree of freedom in the sensor's geometrical design

Why the geometry is of considerable practical importance is illustrated in Fig 8 with a one-dimensional intensity distribution of light $I(x)$ (generated, for example, by employing a cylindrical lens) impinging on a photosensitive structure with spatially varying width $w(x)$ The generated photoresponse L_w is

$$L_w = \int_a^b I(x)w(x)\,dx \tag{2}$$

From this it is concluded that any linear (one-dimensional, parameterized) transform

$$L_f = \int_a^b I(x)f(x)\,dx \tag{3}$$

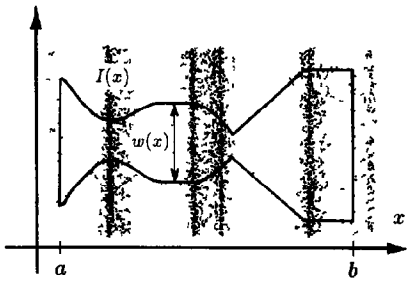

Fig 8 Illustration of the concept of 'optically calculating' one-dimensional, parameterized linear transforms of arbitrary light distributions $I(x)$, by employing a photodiode with an appropriate width profile $w(x)$

can be calculated optically with just two photosensitive structures realizing the positive and negative parts of $f(x)$ with corresponding widths $w^+(x)$ and $w^-(x)$, given by

$$w^+(x) = \begin{cases} f(x) & \text{if } f(x) > 0 \\ 0 & \text{elsewhere} \end{cases} \quad (4a)$$

$$w^-(x) = \begin{cases} -f(x) & \text{if } f(x) < 0 \\ 0 & \text{elsewhere} \end{cases} \quad (4b)$$

so that subtraction of the two photoresponses yields the sought linear transform

$$L_f = \int_a^b I(x)w^+(x)\,dx - \int_a^b I(x)w^-(x)\,dx \quad (5)$$

A simple application of this general technique is the fast optical determination of the centroid This can either be achieved with a PSD as described in Section 3, or by a wedge-shaped photodiode [4] with $w(x) = ax$ This principle has been used for the realization of a triangulation-based 3D (depth) camera, capable of delivering 50 depth maps per second in the form of an intensity-coded standard CCIR video signal [29] Its essential part is an array of wedge-shaped photodiodes (Fig 9(a)) with which the centroid of a light profile is determined optically and completely in parallel Two wedge-shaped photodiodes are used per centroid measurement to obtain (i) the lateral position of the intensity profile, and (ii) the local light intensity at this position Figure 9(b) documents that such an array of wedge-shaped photodiodes can be obtained not only by manufacturing it this way, but also by converting a commercially available array of long rectangular photodiodes to the desired structure with a suitable opaque mask

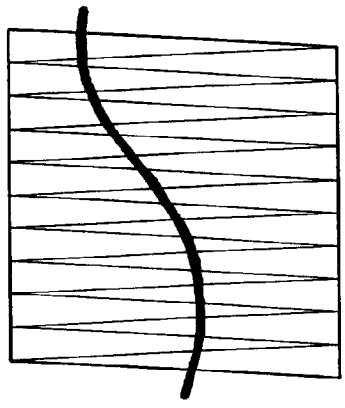

(a)

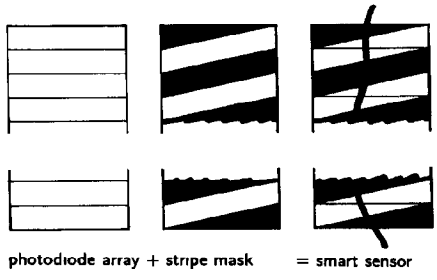

(b)

Fig 9 Array of wedge-shaped photosensors for the optical determination of the centroid of a light-intensity profile (a) Two wedge-shaped photosensors form a pair with which the lateral position (centroid) and the local light intensity of the profile can be measured (b) Such a centroid array can also be produced with a commercially available array of rectangular photosensors and an opaque stripe mask, glued at an angle on top of the sensor

The wedge-shaped centroid detector described above allows the realization of a very simple motion detector, based on detecting temporal variations of the centroid signal Figure 10 shows the block diagram of such a motion detector, usable in such diverse applications as automatic door openers, intrusion detection, presence monitoring for illumination and air-conditioning control, mechanical activity control for machinery, detection of absence of motion (e g , 'baby monitoring') etc The simple scheme in Fig 10 does not employ normalization for changing ambient lighting conditions, such changes are also interpreted as 'motion', so that this sensor should be called more appropriately a 'change detector' Our practical experience with such a motion or change detector (to be described in another publication) indicates that the simple scheme and its implementation

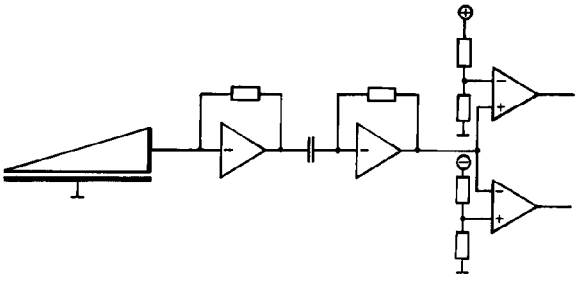

Fig 10 Schematic block diagram of a simple motion or change detector It consists of a wedge photodiode (beneath a cylindrical lens) that determines the optical centroid in one dimension The centroid current signal is first amplified with a transimpedance amplifier, then differentiated and finally the differentiated signal is compared with a positive and a negative threshold signalling either no movement or a movement to the right or the left

work well with sufficient ambient lighting, being much easier to realize than other motion detectors described in the literature [30] In low-light-level environments the gain of the transimpedance amplifiers has to be so high that amplifier offset problems make it necessary to resort to a more complex system, less competitive with other solutions [30]

Another example of an 'optically computed' linear transform is seen in the lower left corner of Fig 5(a), where sinusoidal photodiodes are used to determine the (complex) Fourier coefficients (amplitude and phase) of a one-dimensional light distribution at a fixed spatial frequency This is accomplished by giving the photosensors the correct shape and the use of simple analog electronics A data rate of several MHz can be attained, limited by the response time of the photodiodes

As a last application, we mention a simple passive focus sensor, consisting of a circular arrangement of photodiodes, read out sequentially The sharper the local image content is, the larger is the high-frequency content of the resulting signal By (mechanically) moving the focus position of the lens and letting the sensor continually measure frequency contents of the electrical signal, the point of best focus is determined as the position with maximum high-frequency content The simple focus sensor we realized consists of only eight photodiodes, sufficient to obtain a rough measure for best focus position Better focus sensors contain more photodiodes, but they employ essentially the same basic idea [31]

7. Discussion

We investigated a standard industrial CMOS process for its suitability to integrating optical metrology systems on a single chip We found that the electro-optical performance of the used CMOS process, available through an inexpensive multi-project wafer service, was excellent In addition, we demonstrated the integration of IR and visible light sources (silicon LEDs) with the same process, albeit with very low efficiency

From the excellent results obtained in this investigation, we conclude that integrated optical metrology using fast and cheap CMOS processes is a viable alternative to assembling such a system from commercially available optical and electronics parts Multi-project wafer services offer fast turn-around times of a few weeks and surprisingly low prices for prototype chips With the availability of inexpensive PC-based design, layout and simulation software packages, producing smart optical sensors and 'seeing chips' for special applications is within the reach of everybody with a background in electronics

Acknowledgements

This work would not have been possible without the help and continuing support of Dr R Horisberger (Paul Scherrer Institute, Villigen) in designing and manufacturing sensors and electronic circuitry in silicon ICs We would like to thank him for his enthusiasm and help

Several measurements of the spectra of silicon LEDs emitting in the visible were carried out by Dr E F Steigmeier and H Auderset (Paul Scherrer Institute Zurich) to whom we are very grateful We also acknowledge many interesting discussions about visible light emission from silicon with our two colleagues

Finally we would like to thank Dr H C Sigg (Paul Scherrer Institute, Zurich) for his support and guidance in optically characterizing the IR-emitting silicon LEDs with his Fourier transform IR spectrometer

References

1 C Koch, Seeing chips analog VLSI circuits for computer vision *Neural Comput*, *1* (1989) 184–200

2 M A Mahowald and C Mead, The silicon retina, *Sci Am*, (May)(1991) 40–46
3 C Koch, Implementing early vision algorithms in analog hardware, *Proc SPIE, Vol 1473*, 1991, pp 2–16
4 J Kramer, P Seitz and H Baltes, Photo-ASICs integrated circuits for optical measurements using industrial CMOS technology, *Proc 6th Int Conf Solid-State Sensors and Actuators (Transducers '91) San Francisco, CA, USA, June 24–28, 1991*, pp 727–729
5 FASELEC AG, Binzstrasse 44, CH-8045 Zurich Tel +41-1-465-1111
6 M Bleicher, *Halbleiter-Optoelektronik*, Alfred Huthig Verlag, Heidelberg, 1986, p 98
7 Y Morikawa and K Kawamura, A small distortion two-dimensional position-sensitive detector (PSD) with on-chip MOSFET switches, *Proc 6th Int Conf Solid-State Sensors and Actuators (Transducers '91) San Francisco, CA, USA, June 24–28, 1991*, pp 723–726
8 W S Boyle and G E Smith, Charge coupled semiconductor devices, *Bell Syst Tech J*, *49* (1970) 587–593
9 D F Barbe (ed), *Charge-Coupled Devices, Topics in Applied Physics*, Vol 38, Springer, Berlin, 1980, pp 25–142, 165–166
10 J Janesick, T Elliott, A Dingizian, R Bredthauer, C Chandler, J Westphal and J Gunn, New advancements in charge-coupled device technology—sub-electronic noise and 4096 × 4096 pixel CCDs, *Proc SPIE, Vol 1242*, 1990, pp 223–237
11 Y T Chan, B T French and P E Green, Extremely high speed CCD analog delay line, *Proc 1975 Int Conf Applic CCD, San Diego, CA, USA, 1975*, pp 389–398
12 Orbit Semiconductor Inc, 1230 Bordeaux Drive Sunnyvale, CA 94089, Tel 408-744-1800, FAX 408-747-1263
13 M F Tompsett, G F Amelio, W J Bertram, R R Buckley, W J McNamara, J C Mikkelsen and D A Sealer, Charge-coupled imaging devices experimental results, *IEEE Trans Electron Devices, ED-18* (1971) 992–996
14 C R Hoople and J P Krusius, Characteristics of submicrometer gaps in buried-channel CCD structures, *IEEE Trans Electron Devices, ED-38* (1991) 1175–1181
15 E R Fossum Charge-domain analog signal processing for detector arrays, *Nucl Instrum Methods Phys Res A, 275* (1989) 530–535
16 F J L Sangster and K Terr, Bucket-brigade electronics—new possibilities for delay, time-axis conversion, and scanning, *IEEE J Solid-State Circ*, *SC-4* (1969) 131–136
17 L Boohstra and F J L Sangster, Progress in bucket-brigade charge transfer devices, *Proc IEEE Int Solid-State Circ Conf*, *Philadelphia, PA, USA, 1972*, pp 140–141
18 P K Weimer, M G Kovac, F V Shallcross and W S Pike, Self-scanned image sensors based on charge transfer by the bucket-brigade method, *IEEE Trans Electron Devices, ED-18* (1971) 996–1003
19 Y P Varshni, Band-to-band radiative recombination in groups IV, VI and III–V semiconductors (I), *Phys Status Solidi, 19* (1967) 459–512
20 R Newman, Visible light from a silicon p–n junction, *Phys Rev*, *100* (1955) 700–703
21 A G Chynoweth and K G McKay, Photon emission from avalanche breakdown in silicon, *Phys Rev*, *102* (1956) 369–376
22 L W Davies and A R Storm, Recombination radiation from silicon under strong-field conditions, *Phys Rev*, *121* (1960) 381–387
23 L J Kabell and C J Pecoraro, Silicon avalanche light sources for photographic data recording, in J T Tippett (ed), *Optical and Electro-optical Information Processing*, MIT Press, Boston, MA, 1968, pp 707–714
24 R F Wolffenbuttel and B P van Drieenhuizen, Direct electro-optical actuation in silicon, *Proc 6th Int Conf Solid-State Sensors and Actuators (Transducers '91) San Francisco, CA, USA, June 24–28, 1991*, pp 286–288
25 A S Grove, *Physics and Technology of Semiconductor Devices*, Wiley, New York, 1967, p 195
26 Various authors, *Tech Digest, IEEE Int Electron Devices Meet, Washington, DC, USA, Dec 8–11, 1991*, pp 17–249
27 A G Cullis and L T Canham, Visible light emission due to quantum size effects in highly porous crystalline silicon, *Nature (Lond), 353* (1991) 335–337
28 E Corcoran, Silicon lights up, *Sci Am*, (July) (1991) 86–87
29 J Kramer, P Seitz and H Baltes An inexpensive real-time 3-D camera with a smart optical sensor, *Sensors and Actuators A, 31* (1992) 241–244
30 C Koch, A Moore, W Bair, T Horiuchi, B Bishofberger and J Lazarro, Computing motion using analog VLSI vision chips an experimental comparison among four approaches, *Proc 1991 IEEE Workshop on Visual Motion, Princeton NJ USA, Oct 7–9, 1991*, pp 312–324
31 EG & G Reticon, *Image Sensing Products*, 1989, pp 145–148

Biographies

Jorg Kramer was born in Zurich There he graduated in physics at the Swiss Federal Institute of Technology in 1987 He received an M Sc degree in applied optics from the Imperial College of Science and Technology in 1988, and is now working towards a Ph D at the Paul Scherrer Institute in Zurich His current research interests are in optics and optoelectronics

Peter Seitz was born in Basel, Switzerland He received his M Sc degree in experimental physics (1980) and his Ph D degree (1984) from the Swiss Federal Institute of Technology in Zurich, working at the Institute for Biomedical Engineering This work was in the field of computed tomography, specializing in room-temperature semiconducting X-ray detectors and the mathematics of image reconstruction from incomplete projections In 1984 he joined Laboratories RCA in Zurich, where he worked in the optics and image-processing group In 1987 he transferred to the reorganized laboratory performing high-technology research as part of the Paul Scherrer Institute, where in 1989 he was appointed head of the newly formed image-sensing group His interests centre around solving problems in applied optics and physics, using novel sensors as well as advanced signal- and image-processing techniques

Henry Baltes received the D Sc degree from ETH Zurich in 1971 In the following years he was

on the faculty of the Freie Universitat Berlin, the University of Dusseldorf, the University of Waterloo, Ontario, Canada, and the Ecole Polytechnique Fédérale Lausanne (EPFL)

In 1974, he joined Landis & Gyr Zug Corporation, where he became head of the solid-state device laboratory active in microsensor research From 1975 to 1982, he taught optics, solid-state physics and microsensors at EPFL

From 1983 to 1988, he held the Henry Marshall Tory Chair at the University of Alberta, Edmonton, Canada, where he directed a research program in microsensors As acting president of the Alberta Microelectronic Centre, he was in charge of the establishment of a CMOS fabrication facility From 1986 to 1988, he also was a director of LSI Logic Corporation of Canada

Since 1988 he has been professor of physical electronics at ETH Zurich and head of ETH's Physical Electronics Laboratory active in silicon microsensors In 1991, he joined the Board of Directors of Ascom Microelectronics and was appointed director of the Swiss Federal Priority Program LESIT

Professor Baltes is an associate editor of *Sensors and Materials* and the *Journal of Micromechanics and Microengineering* He is a member of the IEEE, the Optical Society of America, the Institute of Physics, the Electrochemical Society, the Swiss Information Technology Society, the Swiss Electrotechnical Association, the Swiss Society for Sensor Technology and the Swiss Physical Society He has authored or coauthored over 250 publications in scientific or technical journals, 15 patents and four books